

Appendix A

Toroidal Polarimeter Design

The two-arm polarimeter allows excellent cancellation of biases in polarization measurements. The toroids have little fringe field in the beam region and yet provide a large field integral for the pions. The result is a compact two arm device where one arm fits between the two RHIC rings and is upgradable to provide for possible up and down asymmetry measurements in case of radial polarization of the beam at the polarimeter location.

The toroidal design also naturally covers the required energy range without the need for adjusting magnet and detector positions. In the original dipole polarimeter we located the magnet at 30 m from the target and at 6.4 mrad angle for $p_{beam} = 250$ GeV/c; the magnet was relocated to 9.5 m and 64 mrad angle for $p_{beam} = 25$ GeV/c. Such readjustment of polarimeter position at the low energy was necessary in order to maintain a similar solid angle and rate. For a detector at a fixed distance from the target, the coverage in $\Delta\phi/2\pi$ is inversely proportional the scattering angle. However, for the toroids, scattered pions are bent in the r - z plane maintaining constant ϕ . At the lower energy it is possible to transport the pions scattered at 64 mrad to a detector at 30 m, maintaining the same coverage in $\Delta\phi/2\pi$ as for higher energy. Thus, with the toroidal design, it is only necessary to adjust the toroid fields to cover the full energy range and magnets and detectors do not move.

The layout of one polarimeter system is shown in Fig. A.1. Pions are produced by the interaction of polarized protons on a 5 μ m carbon fiber target about 1.5 m downstream of Q4. A string of four toroids surrounds the warm beam line section between Q4 and Q3. The first toroid is 3 m long, the second and third are 1.5 m long all of the same cross-sectional geometry. The fourth toroid is 6 m long and its bore radius is 3 cm larger than that of the first three. The latter allows for placement of heating pads around the beam pipe. The inter-magnet drift regions of 1.4 m are for possible placement of collimators and detectors. This arrangement provides enough space for a collimator and a 6 m long Cerenkov counter as well as tracking detectors. If necessary a hadron calorimeter may be placed downstream of the Cerenkov counter. Each polarimeter has four arms that may be used to measure left-right and up-down asymmetry. The limited space between the two RHIC rings constrains detector sizes.

The production angle and selected spectrometer momentum depend on the beam energy; at RHIC

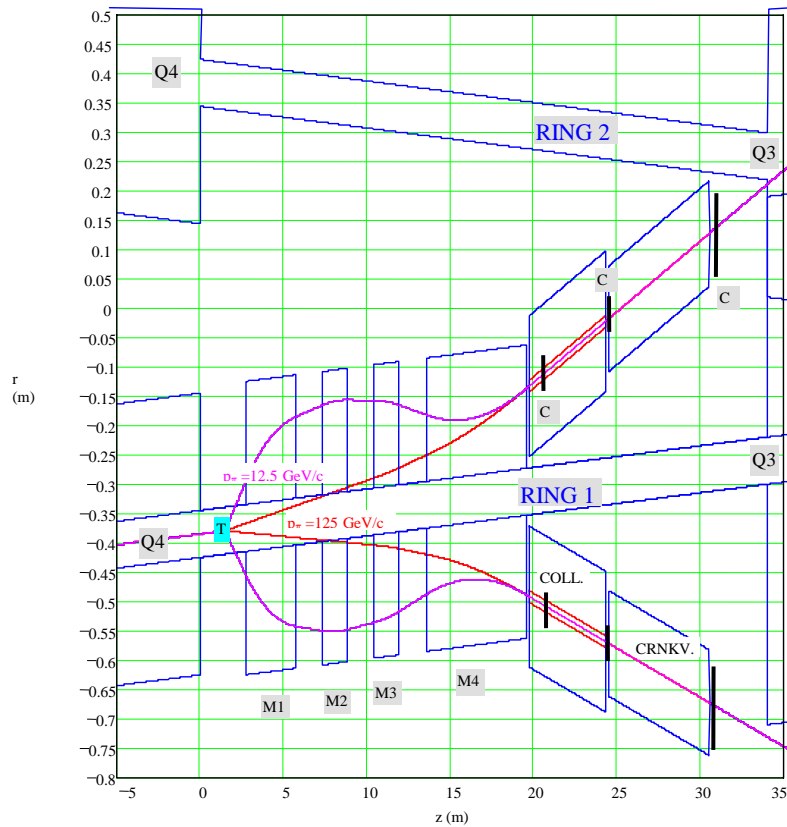


Figure A.1: Plan view of the the two-arm polarimeter between Q4 and Q3 including the two RHIC beam lines. The two trajectories shown were calculated assuming hard edged magnets. The total bend angles for the 25 GeV/c and the 250 GeV/c tunes are 46 mrad and 12 mrad, respectively.

	Trgt	M1	M2	M3	M4	Coll.	CrnkV
Position (m)	1.5	2.75	7.35	10.45	3.55	19.75	24.55
Length (m)	0	3	1.5	1.5	6	4.6	6
23 GeV/c		-1	-1	-0.85	+0.380		
25 GeV/c		-0.99	-0.65	-0.4471	+0.3321		
100 GeV/c		-0.2	-1	-0.9	+0.782		
200 GeV/c		0	0	-0.275	+0.94		
250 GeV/c		0	0	+0.9	+0.9		

Table A.1: Parameters for the polarimeter layout. The positions of the elements are with respect to the end of Q4. The magnet settings are in fractions of the TOSCA design fields in Fig. A.3.

injection of 25 GeV/c, the production angle would be 64 mrad and the π momentum 12.5 GeV/c; at 250 GeV/c RHIC beam momentum, the production angle is 6.4 mrad and the π momentum is 125 GeV/c. For the smallest angle, 6.4 mrad, the spectrometer magnets will be set for near maximum deflection so that detectors behind the 2 cm slit collimator are shielded from straight-through neutrals. This fixes the positions of the collimator, the Cerenkov counter and all other possible detectors downstream of the collimator. For all other beam momenta, including injection at about 25 GeV/c, the four toroids can be set to guide pions with $x_F = 0.5$ and $p_T = 0.8$ GeV/c through the collimator. The apparatus thus allows measurement at various beam momenta without major readjustments to the detector positions. The details of the layout in Fig. A.1 are listed in Table A.1. The table also includes possible tunes at selected beam energies that will allow measurement in the desired kinematic range of $x_F = 0.5$ and $p_T = 0.8$ GeV/c.

A.1 Toroidal Magnets, Pion Exit Windows

Each toroid consists of four pie-shaped pole pieces with a 7° angular opening between adjacent poles (see Fig. A.2). The right and left arms measure vertical polarization, and, if necessary the steel wedges can be removed from the up and down arms and, with proper instrumentation, may be used to measure radial polarization. Several options were considered in the design of the toroidal magnets, and the parameters of a 2-dimensional TOSCA design are indicated in Table A.2. Bipolar power supplies are necessary for measurements with positive as well as negative pions and for flexibility in tuning. In order to achieve sufficient integrated field strength the beam pipe diameter was chosen to be 8 cm. Fig. A.3 shows the radial and azimuthal field configurations in the middle of the two types of magnets. Note that there are strong radial fields near the coil positions.

The four openings break the toroidal symmetry and give rise to octupolar fringe fields inside the RHIC beam pipe. The amplitude of the field at a radius of 1 cm is about 6 Gauss. A 5 mm thick iron shielding reduces the amplitude by more than a factor of 20 and the perturbation to the RHIC beam is negligible [77].

Multiple Coulomb scattering at the pion exit windows is an important issue that impacts the accuracy of track reconstruction. Even though the detailed mechanical design has not yet been completed, we envision providing a single thin window or set of multiple thin windows (3 mil Aluminum) over the 6 m section of the beam line spanning the pion production angles of 64 to 6.4 mrad. For a 3 mil aluminum window the multiple scattering angles are 0.13 mrad and 0.04 mrad at pion momenta of 12.5 GeV/c and 125 GeV/c, respectively. The multiple scattering angle is significantly less than the pion production angle and the bend angle by the spectrometer. The expected multiple scattering angles at the exit window are thus tolerable. The multiple window option carries the risk of not being able to measure the polarization at some energies where the desired production angle happens to take the pions through the thick sections of the beam pipe.

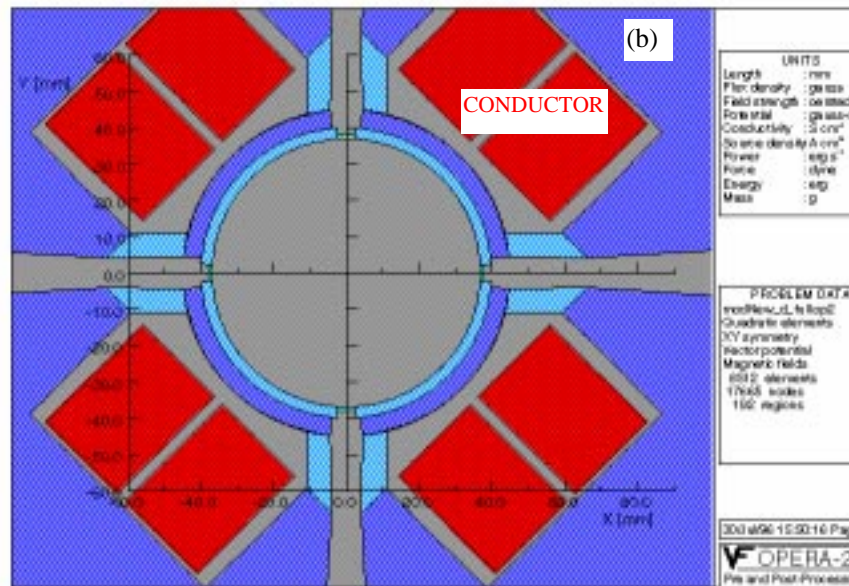
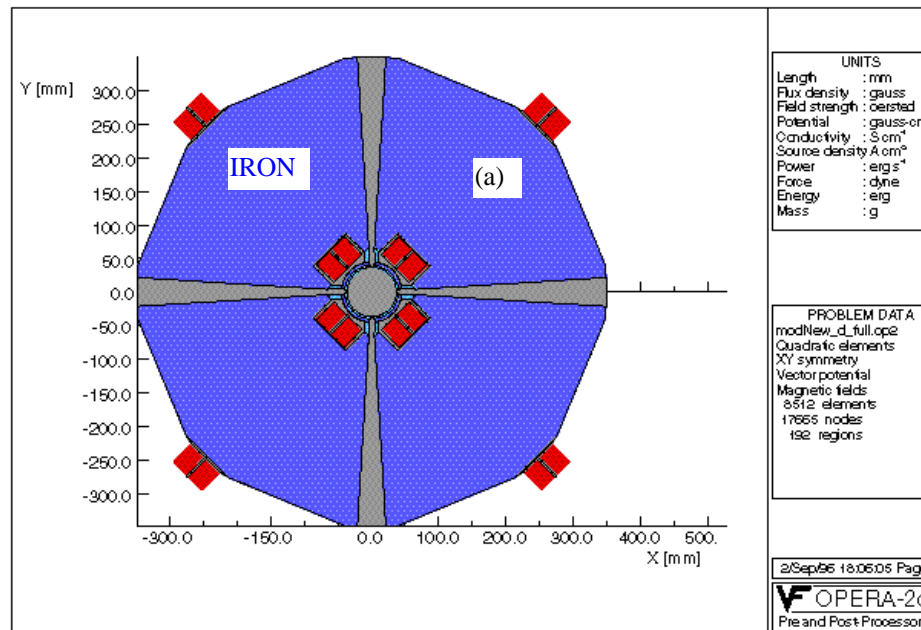


Figure A.2: Cross-sections of the toroidal magnets. The iron shield around the beam pipe reduces the field leakage by more than a factor of 20.

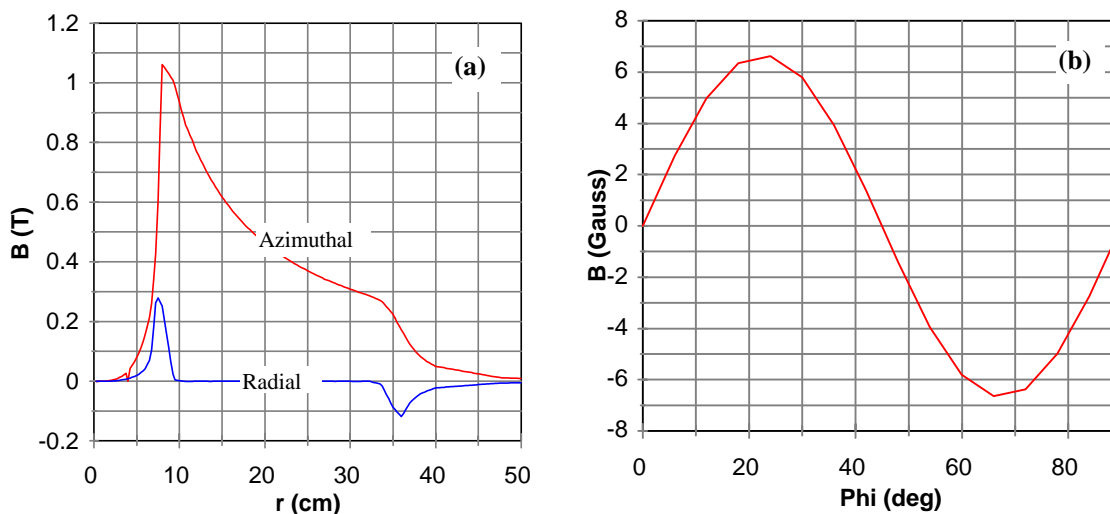


Figure A.3: (a) Expected azimuthal and radial magnetic field strength within the gaps in the toroid. The azimuthal field varies very little from the mid-plane to the half-angle limit of 3.5° . The radial field vanishes at the mid-plane and changes sign between the upper and lower halves of the 7° opening; the radial field plot shown is for a plane at 3° from the mid-plane. (b) The radial component of the leakage field inside the beam pipe at $r=1$ cm, as function of azimuthal angle with no magnetic shielding.

Turns per quadrant	31
Copper Conductor	9 mm \times 9 mm, 5 mm hole
Max. Current Density	550 A/cm ²
Max. Current	332 A
Voltage	41 V for $L = 1.5$ m; 52 V for $L = 2$ m
Power Supply (bipolar)	15 KW for $L = 1.5$ m; 17 KW for $L = 2$ m

Table A.2: Parameters for a preliminary design of a toroidal magnet. Voltage specifications were estimated assuming that there will be no field ramping requirements.

p_{beam} (GeV/c)	Luminosity ($\text{cm}^{-2}\text{s}^{-1}$)	$N_{\pi/bunch}$	T_{meas} (sec)	$\Delta\epsilon_x$ ($\Delta\epsilon_y$) (π mm mrad)
250	4.5×10^{34}	5×10^{-4}	3.2	0.012 (0.013)
25	1.4×10^{34}	1.5×10^{-5}	7.2	0.8 (1.2)

Table A.3: Acceptance and rate estimates for the toroidal polarimeter. Also includes expected emittance dilution due to multiple scattering for collecting 10^4 pions. The following parameters were assumed: $\epsilon_N = 20\pi$ mm mrad, protons/fill = 120 bunches at 2×10^{11} protons/bunch, $d_f = 2.5 \times 10^{-8}$ m, $d_w = 10\mu$ m, $p_T = 0.8$ GeV/c, $\delta p/p = 0.1$.

A.2 Pion Production Target

The toroid design utilizes the same production target as was described in Section 8.3.2.

A.3 Acceptance, Event Rates and Emittance Blowup

We define ϕ as the angle between the magnet mid-plane and the pion production plane. For pions traversing the magnet gaps between the inner conductors, the ϕ -acceptance is determined by the strength and direction of the radial fields which are significant only near the conductor positions (see Fig. A.3). These fields are defocusing in ϕ if the polarity of the magnet is set to be radially focusing as is the case for the first three magnets in the 25 GeV/c tune. The position of the first magnet in Fig. A.1 was optimized such that pions with $p_L = 12.5$ GeV/c and $p_T = 0.8$ GeV/c do not pass between the inner magnet coils. Instead they enter the first magnet at $r > 8$ cm beyond which the radial fields are insignificant. This arrangement results in a ϕ -acceptance of about 6.4° . The high energy (125 GeV/c) pions, on the other hand, always have the full ϕ -acceptance of 7° because the radial fields encountered are always focusing in ϕ .

A simple estimate of the expected θ acceptance of the system was made by numerical evaluation of the range of production angles (or p_T) that are accepted by the 2 cm slit collimator. The plots in Fig. A.4 show the acceptance as a function of x_F at the 25 GeV/c and 250 GeV/c tunes. The acceptance is seen to extend to x_F and p_T values below the desired kinematic ranges of 0.5 and 0.8 GeV/c, especially for the high energy case. From the Fermilab and ZGS experiments, significant asymmetries can be expected only above $x_F > 0.45$ and $p_T > 0.7$ GeV/c. It is therefore necessary that the system be able to reject low momentum pions that do not carry significant analyzing power.

With the kinematic acceptance defined as $\delta x_F/x_F$ of 0.1 around x_F of 0.5, and using the p_T acceptance from Fig. A.4(c) we can estimate the event rates. The result is shown in Table A.3.

As in Chapter 8, we estimate the event rates and measuring times of the toroid system. These are listed in Table A.3.

Tracking studies at beam energy of 200 GeV/c have been done. The main concern in this study was the large pion multiplicity resulting from the interaction of one bunch in RHIC intersecting the Carbon target. These cannot be separated in time by electronic means in the polarimeter with either hodoscopes

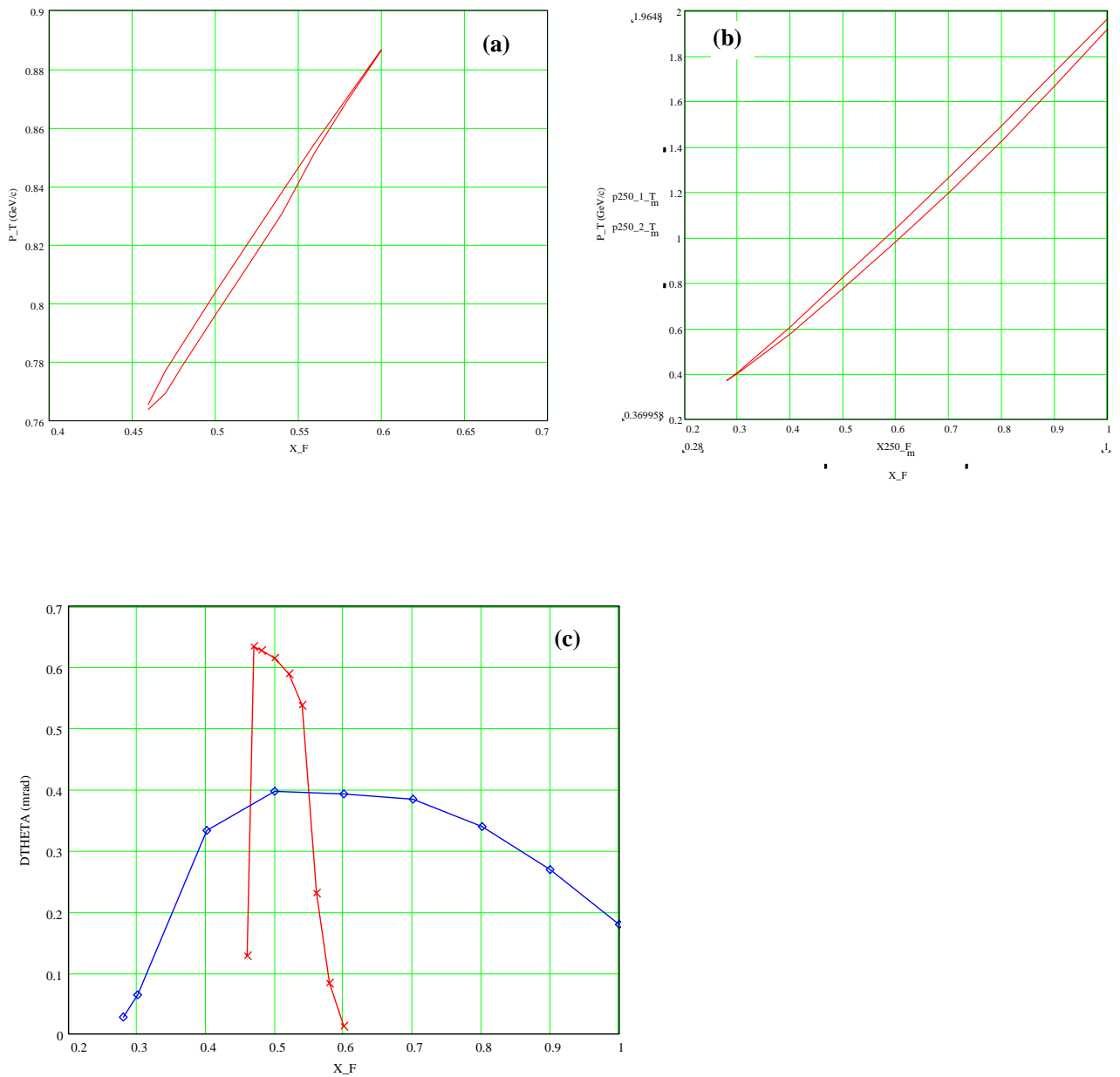


Figure A.4: Polarimeter acceptance for (a) the 12.5 GeV/c and (b) the 125 GeV/c, tunes in Table A.1. (c) The angular acceptance in the mid-plane derived from (a) and (b).

or calorimeter. The number of interactions in one crossing of the bunch with 5 μm target is of order 10^4 . However, the planned Carbon ribbon target has a factor 500 lower collision rate. Simulations showed acceptable rates as for Chapter 8.

A.4 Polarimeter Detectors

The detectors will determine the (x_F, p_T) for each particle, and crudely measure the energy of each particle. If π^+ measurement becomes feasible, the Cerenkov counter will be used to identify pions. The (x_F, p_T) measurement will allow selection of pions with high analyzing power. We will want to choose pions with $x_F > 0.47$ and $p_T > 0.7$ GeV/c (see Fig. 8.1)[78]. The acceptance of the toroids and collimator extends to lower (x_F, p_T) where pion production is significantly larger (see Fig. A.4) and the analyzing power lower. Therefore, the lower edge of (x_F, p_T) for the selected pions must be sharply defined. Particle identification (π^+ from p) is required for positives, although we may decide to use only π^- if the analyzing power for π^- production at the RHIC injection energy is found to be large in AGS experiment E925. We plan to use tracking to measure (x_F, p_T) and, in addition, hadron calorimeters to provide a cruder but independent measurement of the pion energy.

An important detector issue is to isolate the detectors out of the line of sight of the target. For this reason the collimator points downstream of the target, and the detectors will be downstream of the collimator. Therefore, to reconstruct the pion trajectories we use the target/beam location as an upstream point, and we measure the deflection (r) and track angle (Θ_{meas}) after the bending in the toroids, downstream of the collimator, (see Fig. A.1).

We plan to measure x_F to $\delta x_F = \pm 0.02$ and p_T to $\delta p_T = \pm 0.03$ GeV/c, which is similar to the E704 resolution. The binning in the E704 data was $\Delta x_F = 0.05$ and $\Delta p_T = 0.07$ GeV/c (full width). The δp_T resolution requires detection resolution of $\delta r = \pm 1.6$ mm and $\delta \Theta_{meas} = \pm 0.11$ mrad. The δx_F resolution requires similar resolution for Θ_{meas} and less stringent δr . The magnetic field integral should be known to $\delta p_{kick}/p_{kick} = \pm 0.02$, and the location of the bend center should be known to $\delta L_{bend}/L_{bend} = \pm 0.02$ so that these give negligible contributions.

The target point is defined by the beam width, and $\delta x_{target} = \pm 0.8$ mm at 200 GeV/c. We use an emittance of 20π mm-mrad and $\beta_x = 36$ m and $\gamma_x = 0.09$ m $^{-1}$. (We will use a radial carbon ribbon target with the pion source width defined by the beam radially. We can then bin the beam polarization vertically to measure any polarization dependence on y .) Therefore, the target source location will contribute a negligible error to δr . The beam radial divergence is $\delta \Theta_{r,beam} = \pm 0.04$ mrad, also contributing negligible error in $\delta \Theta_{meas}$.

Multiple Coulomb scattering in the pion exit window (0.003 inch/ Θ_{prod} , aluminum) and 30 m of air give $\delta \Theta_{mult} = \pm 0.04$ mrad and $\delta r_{mult} = \pm 1$ mm at the location of the first tracking module, 25 m from the exit window, for 200 GeV/c beam (100 GeV/c pions).

We plan to use either wire chambers or scintillator hodoscopes with 2 mm pitch, and x , y , and u

planes for tracking. Three tracking modules will be spaced over 10 m, each covering an area of $3 \times 3 \text{ cm}^2$. Resolution will be $\delta r_{meas} = \pm 1 \text{ mm}$ and $\delta \Theta_{meas} = \pm 0.1 \text{ mrad}$, which satisfies the requirements above. If scintillator were used, 9 mm of scintillator in the first tracking module would give $\delta \Theta_{mult} = \pm 0.02 \text{ mrad}$.

We have not designed the tracking modules at this time. For wire chambers, the drift time should be $< 100 \text{ nsec}$, the bunch spacing in RHIC for 120 bunches per ring. The multiplicity downstream of the collimator is expected to be 0.0035/plane/bunch crossing for π^- , so that the granularity, 10 to 15 pixels/plane, is sufficient. We expect to use deadtimeless pipeline readout, and store the data during the measurement time. After the measurement, fast arithmetic processors can reconstruct the straight line tracks, obtaining (r, Θ_{meas}) for each event. A look-up table can then locate the event in (x_F, p_T) . The data would then be binned according to the bunch polarization sign pattern in the ring, and polarimeter arm. The asymmetry is calculated similarly to the AGS internal polarimeter. Finally, the beam polarization is calculated using the known analyzing power. We expect that the processing time will be short, giving essentially instantaneous beam polarization information.

We plan to use a hadron calorimeter after the tracking modules. We do not have the space to completely contain the energy on the sides, so that we expect a resolution of $\delta E/E = (\pm 100\%)/\sqrt{E}$, or $\pm 10\%$ at 200 GeV/c beam (100 GeV/c pions). This will give an independent measurement of the energy, and provide both a cross-check of the tracking and a separate measure of the beam polarization without the track reconstruction. Both the Cerenkov and the calorimeter require that only one high energy track be in the acceptance.

